Published in final edited form as:
J Biomed Mater Res B Appl Biomater. 2012 July ; 100(5): 1378–1386. doi:10.1002/jbm.b.32709.

Effect of amorphous calcium phosphate and silver nanocomposites on dental plaque microcosm biofilms

Lei Cheng[1,2], **Michael D. Weir**[1], **Hockin H. K. Xu**[1], **Joseph M. Antonucci**[3], **Nancy J. Lin**[3], **Sheng Lin-Gibson**[3], **Sarah M. Xu**[1], and **Xuedong Zhou**[2]

[1]Biomaterials & Tissue Engineering Division, Department of Endodontics, Prosthodontics and Operative Dentistry, University of Maryland Dental School, Baltimore, Maryland 21201

[2]State Key Laboratory of Oral Diseases, West China College of Stomatology, Sichuan University, Chengdu, China

[3]Biomaterials Group, Polymers Division, National Institute of Standards & Technology, Gaithersburg, Maryland 20899

Abstract

A dental composite containing amorphous calcium phosphate nanoparticles (NACP) was developed that released calcium (Ca) and phosphate (PO_4) ions and possessed acid-neutralization capability. There has been little study on incorporation of antibacterial agents into calcium phosphate composites. The objective of this study was to investigate the effect of silver nanoparticle (NAg) mass fraction in NACP nanocomposite on mechanical properties and dental plaque microcosm biofilm for the first time. NACP nanoparticles of 116 nm were synthesized via a spray-drying technique. NAg nanoparticles were synthesized using Ag 2-ethylhexanoate and 2-(*tert*-butylamino)ethyl methacrylate, yielding NAg of particle size of 2.7 nm that were well-dispersed in the resin. Five NACP nanocomposites were fabricated with NAg mass fractions of 0, 0.028, 0.042, 0.088, and 0.175%, respectively. Mechanical properties of NACP nanocomposites containing 0–0.042% of NAg matched those of a commercial composite without antibacterial activity. Live/dead assay of dental plaque microcosm biofilms showed complete coverage with live bacteria on commercial composite. However, there were increasingly more dead bacteria with higher NAg content in the NACP nanocomposite. Colony-forming unit (CFU) counts for total microorganisms, total Streptococci, and mutans Streptococci for NACP nanocomposite with 0.042% NAg were about 1/4 those of commercial composite. Lactic acid production on NACP nanocomposite with 0.042% NAg was 1/3 that on commercial composite. In conclusion, novel NACP–NAg nanocomposites were developed which possessed good mechanical properties and potent antibacterial properties, with substantially reduced biofilm viability and lactic acid production. Hence, the NACP–NAg nanocomposites are promising for dental restorations with remineralizing and antibacterial capabilities.

Keywords

antibacterial nanocomposite; amorphous calcium phosphate nanoparticles; silver nanoparticles; human dental plaque microcosm biofilm; stress-bearing; tooth caries inhibition

Correspondence to: H. H. K. Xu; hxu@umaryland.edu.

INTRODUCTION

Dental resin composites are being increasingly used as restorative materials, core buildup materials, inlays, onlays, crowns, cavity liners, and pit and fissure sealants.[1] Extensive studies have resulted in significant improvements in filler and polymer matrix compositions as well as curing and handling characteristics.[2–7] One major drawback, however, is that composites tend to accumulate more biofilm and plaque *in vivo* than other restorative materials.[8–11] Such plaque accumulation with acid production by acidogenic bacteria could result in secondary caries. Indeed, recurrent caries at restoration margins is cited as a main reason for replacing the existing restorations.[12–14] Overall, about half of dental restorations fail within 10 years, and replacing them consumes 60% of the average dentist's practice time.[15–17] Replacement dentistry in the USA costs $5 billion annually.[18]

Composites with remineralizing capabilities via calcium phosphate (CaP) particles as a portion of the filler phase have been developed.[19–22] Previous studies showed that these composites released supersaturating levels of calcium (Ca) and phosphate (PO_4) ions and remineralized tooth lesions *in vitro*.[20,22] These composites contained traditional CaP particles with sizes of several microns to tens of microns.[19,20,22] Novel nanoparticles of CaP and CaF_2 were recently synthesized with sizes of about 50–100 nm and were incorporated into dental composites.[21,23] In particular, nanoparticles of amorphous calcium phosphate (NACP) were synthesized with a mean particle size of 116 nm.[24] The NACP composite released Ca and PO_4 ions at levels similar to those of previous CaP composites, but with a 2-fold increase in mechanical properties.[23,24] In addition, the NACP composite was "smart" and greatly increased Ca and PO_4 ion release at acidic pH, when these ions were most needed to combat caries.[24] Furthermore, NACP composite possessed a unique acid neutralization capability.[25] It neutralized a lactic acid solution of pH 4 and increased the pH to a safe level of 6, while the commercial restoratives had pH remaining at 4.[25] It is desirable for the NACP composite to further possess strong antibacterial properties. However, to date there has been little study on development of antibacterial CaP composites.

Silver (Ag) is antibacterial, antifungal, and antiviral.[26,27] Ag-containing silica particles were used as fillers to develop antibacterial composites.[28,29] Ag-containing composite inhibited *Streptococcus mutans* (*S. mutans*) growth, and appeared to have a long-lasting antibacterial effect.[29] Ag nanoparticles (NAg) demonstrated a high antibacterial efficacy.[30] Dental composites containing NAg had a strong antibacterial property.[31,32] An advantage of NAg is their high surface area to mass ratio, such that a small amount of NAg is sufficient for the composite to be strongly antibacterial, without significantly compromising the composite color or mechanical properties.[32] Recently, a nanocomposite was developed with well-dispersed NAg at a low NAg mass fraction of 0.08%.[32] Such a low NAg filler level would minimize the impact on esthetics, handling and mechanical properties of the composite, while reducing the *S. mutans* coverage by about half.[32] However, a single NAg mass fraction was used in that study, and no CaP fillers were used in that composite. There has been no report on the effect of different NAg concentrations on the antibacterial properties of CaP composite.

The objective of this study was to develop novel nanocomposites containing nanoparticles of both NACP and NAg to achieve caries-inhibiting capabilities. The rationale for the composite was to not only have a remineralizing capability due to the NACP fillers, but also to a potent antibacterial capability due to NAg. It was hypothesized that (1) incorporating NAg in NACP nanocomposite would achieve strong antibacterial properties as evaluated using a dental plaque microcosm biofilm model; (2) higher NAg mass fractions in the composite would result in lower biofilm viability, metabolic activity, and lactic acid production; (3) adding NAg to the NACP nanocomposite would not compromise the

mechanical properties, which would match those of a commercial composite control without antibacterial capability.

MATERIALS AND METHODS

NACP and NAg nanocomposites

The synthesis of NACP, $Ca_3(PO_4)_2$, was recently described.[24,25] Briefly, a spray-drying technique was used. Calcium carbonate and dicalcium phosphate anhydrous were dissolved into an acetic acid solution to obtain Ca and PO_4 ionic concentrations of 8 and 5.333 mmol/L, respectively, yielding a Ca/P molar ratio of 1.5. This solution was sprayed into a heated chamber, and an electrostatic precipitator was used to collect the dried particles. This method produced NACP with a mean particle size of 116 nm.[24]

A resin of BisGMA (bisphenol glycerolate dimethacrylate) and TEGDMA (triethylene glycol dimethacrylate) at 1:1 mass ratio was rendered light-curable with 0.2% camphorquinone and 0.8% ethyl 4-*N*,*N*-dimethylaminobenzoate (all mass% unless otherwise noted). Silver 2-ethylhexanoate was dissolved into 2-(*tert*-butylamino) ethyl methacrylate (TBAEMA, Sigma, St. Louis, MO) by gentle stirring, which was then added to the BisGMA–TEGDMA resin. To prepare 0.08% mass fraction of Ag salt in the resin, 0.08 g of silver 2-ethylhexanoate was dissolved into 1 g of TBAEMA.[32] Then, 1% of this solution was added to the BisGMA–TEGDMA resin. TBAEMA was used because it improved the solubility by forming Ag–N coordination bonds with Ag ions, thereby facilitating the Ag salt to dissolve in the resin solution. In addition, TBAEMA contains reactive methacrylate groups and can be chemically incorporated into the polymer network upon photo-polymerization.[32] By using different Ag salt amounts, five different BisGMA–TEGDMA–Ag resins were prepared at silver 2-ethylhexanoate mass fractions of 0, 0.08, 0.12, 0.25, and 0.50%, respectively. The 0.08% was used following the previous study,[32] and mass fractions greater than 0.50% were not used due to the diminished mechanical properties.

For each resin, 30% of NACP was used as fillers following a previous study.[25] To obtain load-bearing capability, 35% of barium boroaluminosilicate glass particles of a median diameter of 1.4 μm (Caulk/Dentsply, Milford, DE) were used as co-fillers, which were silanized with 4% 3-methacryloxypropyltrimethoxysilane and 2% *n*-propylamine. The total filler level of 65% yielded a cohesive paste that was readily mixed. The five silver mass fractions in the resin yielded a final silver 2-ethylhexanoate mass/composite mass of 0, 0.028, 0.042, 0.088, 0.175%, respectively.

Hence, five NACP-containing nanocomposites were fabricated and referred to as: (1) NACP + 0% NAg, (2) NACP + 0.028% NAg, (3) NACP + 0.042% NAg, (4) NACP + 0.088% NAg, (5) NACP + 0.175% NAg. A commercial nanocomposite (Renamel, Cosmedent, Chicago, IL) was used as a comparative control. Renamel consisted of nanofillers of 20–40 nm with 60% fillers in a multifunctional methacrylate ester resin.[33] All specimens were photo-polymerized (Triad 2000, Dentsply, York, PA) for 1 min on each side. For mechanical properties, each paste was placed into rectangular molds of (2 × 2 × 25) mm. For biofilm experiments, disk molds of 9 mm in diameter and 2 mm in thickness were used. The disks were sterilized via an ethylene oxide sterilizer (Anprolene AN 74i, Andersen, Haw River, NC).

Transmission electron microscopy

Transmission electron microscopy (TEM; Tecnai T12 high resolution, FEI Company, Hillsboro, OR) was used to examine the silver nanoparticles in the resin. Following a previous study,[32] a thin sheet of mica was partially split and the Ag-containing resin was

placed in the gap. The resin–mica sandwich was pressed with an applied load of 2.7×10^7 *N* to form a thin sheet of resin in between the two mica layers.[32] The resin in the mica was photo-cured for 1 min. The mica sheet was then split apart after 1 day using a scalpel to expose the polymerized film. An ultrathin layer of carbon was vacuum-evaporated onto the composite (Electron Microscopy Sciences, Hatfield, PA). The carbon-coated sample was partial submerged in distilled water to float the thin film onto the water's surface. A copper grid was then used to retrieve the film. After drying, TEM was performed at an accelerating voltage of 120 kV. The NAg sizes were measured using an image analysis software (V600, Advanced Microscopy, Woburn, MA).

Mechanical properties

The composite bars were immersed in distilled water at 37°C for 1 day. Then the specimens were fractured in three-point flexure with a 10-mm span at a crosshead-speed of 1 mm/min (5500R, MTS, Cary, NC). Flexural strength (S) was calculated as $S = 3P_{max}L/(2bh^2)$, where P_{max} is the fracture load, L is span, b is specimen width, and h is specimen thickness. Elastic modulus (E) was calculated as $E = (P/d)(L^3/[4bh^3])$, where load P divided by displacement d is the slope of the load-displacement curve in the linear elastic region.

Saliva collection for biofilm inoculum

Dental plaque microcosm biofilms are laboratory models with the advantage of maintaining much of the complexity and heterogeneity of the dental plaque *in vivo*.[34] Human saliva was shown to be ideal for growing dental plaque microcosm biofilms *in vitro*.[34] The human saliva microcosm model of this study was approved by the University of Maryland. Following a previous study,[35] saliva for biofilm inoculums was collected from a healthy adult donor. The donor had natural dentition without active caries or periopathology, and without the use of antibiotics within the last 3 months. The donor did not brush teeth for 24 h and abstained from food or drink intake for at least 2 h prior to donating saliva. Stimulated saliva was collected during parafilm chewing and kept on ice. The saliva was diluted in sterile glycerol to a concentration of 30%, and stored at −80°C in 2 mL aliquots.[35]

Dental plaque microcosm biofilm formation

The biofilm growth medium contained mucin (type II, porcine, gastric) at a concentration of 2.5 g/L; bacteriological peptone, 2.0 g/L; tryptone, 2.0 g/L; yeast extract, 1.0 g/L; NaCl, 0.35 g/L, KCl, 0.2 g/L; $CaCl_2$, 0.2 g/L; cysteine hydrochloride, 0.1 g/L; hemin, 0.001 g/L; vitamin K1, 0.0002 g/L, at pH 7.0.[36] The saliva–glycerol stock was added, with 1:50 final dilution, into the growth medium as inoculum. 1.5 mL of inoculum was added to each well of 24-well plates, then a composite disk was placed in each well and incubated in 5% CO_2 at 37°C for 8 h. The disks were then transferred to new 24-well plates filled with fresh medium and incubated. After 16 h, the disks were transferred to new 24-well plates with fresh medium and incubated for 24 h. Plaque microcosm biofilms were formed on the disks with this 48 h incubation.[35]

Live/dead bacteria staining

After 48 h growth, the plaque microcosm biofilms on the disks were gently washed three times with phosphate-buffered saline (PBS), and then stained using the BacLight live/dead bacterial viability kit (Molecular Probes, Eugene, OR). Live bacteria were stained with Syto 9 to produce a green fluorescence, and bacteria with compromised membranes were stained with propidium iodide to produce a red fluorescence. Disks were examined using an inverted epifluorescence microscope (Eclipse TE2000-S, Nikon, Melville, NY).

MTT assay of metabolic activity

The MTT (3-[4,5-dimethylthiazol-2-yl]-2,5-diphenyltetrazolium bromide) assay is a colorimetric assay that measures the enzymatic reduction of MTT, a yellow tetrazole, to formazan. After 48 h growth, each composite disk with biofilm was transferred to a new 24-well plate, then 1 mL of MTT dye (0.5 mg/mL MTT in PBS) was added to each well and incubated at 37°C in 5% CO_2 for 1 h. During this process, metabolically active bacteria reduced the MTT to purple formazan. After 1 h, the disks were transferred to a new 24-well plate, 1 mL of dimethyl sulfoxide (DMSO) was added to solubilize the formazan crystals, and the plate was incubated for 20 min with gentle mixing at room temperature in the dark. After mixing via pipetting, 200 μL of the DMSO solution from each well was transferred to a 96-well plate, and the absorbance at 540 nm (optical density OD540) was measured via a microplate reader (SpectraMax M5, Molecular Devices, Sunnvale, CA). A higher absorbance is related to a higher formazan concentration, which indicates a higher metabolic activity in the biofilm on the disk.

Lactic acid production and viable cell counts

After 48 h of biofilm growth, each disk was rinsed with cysteine peptone water (CPW) to remove loose bacteria. The disks were transferred to 24-well plates containing buffered peptone water (BPW) plus 0.2% sucrose. The samples were incubated in 5% CO_2 at 37°C for 3 h to allow the biofilms to produce acid. The BPW solutions were then stored for lactate analysis.

The disks with biofilms were then transferred into tubes with 2 mL CPW, and the biofilms were harvested by sonication and vortexing at the maximum speed for 20 s using a vortex mixer (Fisher, Pittsburgh, PA). Three types of agar plates were used to assess the microorganism viability after serially dilution in CPW. First, tryptic soy blood agar culture plates were used to determine total microorganisms.[35] Second, mitis salivarius agar (MSA) culture plates, containing 15% sucrose, were used to determine total streptococci.[37] This is because MSA contains selective agents crystal violet, potassium tellurite and trypan blue, which inhibit most gram-negative bacilli and most gram-positive bacteria except streptococci, thus enabling streptococci to grow.[37] Third, cariogenic mutans Streptococci is known to be resistant to bacitracin, and this property is often used to isolate mutans Streptococci from the highly heterogeneous oral microflora. Hence, MSA agar culture plates plus 0.2 units of bacitracin per mL was used to determine mutans streptococci.[38] This approach evaluates the antibacterial effect on the total microorganisms in the dental plaque microcosm biofilm, as well as on the mutans Streptococci group which consists of *S. mutans* and *Streptococcus sobrinus, both of which* play a major role in tooth decay by metabolizing sucrose to lactic acid.

Lactate concentrations in the BPW solutions were determined using an enzymatic (lactate dehydrogenase) method according to previous studies.[39] The microplate reader was used to measure the absorbance at 340 nm (optical density OD_{340}) for the collected BPW solutions. Standard curves were prepared using a lactic acid standard (Supelco Analytical, Bellefonte, PA).

Statistical analysis

One-way and two-way analyses of variance (ANOVA) were performed to detect the significant effects of the variables. Tukey's multiple comparison test was used to compare the data at a p-value of 0.05. Each standard deviation (sd) serves as the estimate for the standard uncertainty associated with a particular measurement.

RESULTS

Figure 1 shows a typical TEM image of NAg in the BisGMA–TEGDMA resin. NAg showed as black dots. NAg particle sizes were about 2–4 nm, with (mean ± sd; $n = 100$) of (2.7 ± 0.6) nm. The NAg particles were well dispersed in the resin, without noticeable agglomeration.

Flexural strength (*A*) and elastic modulus (*B*) are plotted in Figure 2. At 0% NAg, the NACP nanocomposite had a flexural strength (mean ± sd; $n = 6$) of (64 ± 7) MPa, not significantly different from the (69 ± 8) MPa of composite control ($p > 0.1$). They are similar to the (68 ± 3) MPa at 0.028% NAg ($p > 0.1$). Increasing the NAg mass fraction to 0.175% markedly degraded the strength ($p < 0.05$). The elastic modulus of NACP composite with 0–0.088% of NAg were similar to, or slightly higher than, the modulus of composite composite control. The modulus at 0.175% NAg was lower than the moduli of all other composites ($p < 0.05$).

Live/dead staining images of biofilms on the composites are shown in Figure 3. Live bacteria were stained green, and dead bacteria were stained red. Yellow/orange colors appeared when the live and dead bacteria were in close proximity. The composite control and NACP with 0% NAg had a thick and continuous biofilm coverage of primarily live bacteria, with occasional dots of dead cells. However, there was a noticeable increase in red/orange staining with increasing the NAg from 0 to 0.028% in the composite, indicating that the NAg rendered the composite antibacterial. The antibacterial potency increased with higher NAg content, and at 0.088 and 0.175% NAg, with a significant increase in red/orange colors in the biofilms.

The biofilm metabolic activity was measured using the MTT assay and plotted in Figure 4. Composite control and NACP nanocomposite without NAg had similar values ($p > 0.1$). There was a monotonic decrease in MTT with increasing NAg content. The metabolic activity on NACP composite with 0.042% NAg was about 1/2 that without NAg. The metabolic activity on NACP composite with 0.175% NAg was decreased by 10-fold, compared to that without NAg.

The CFU counts are plotted in Figure 5 for (A) total microorganisms, (B) total Streptococci, and (C) mutans Streptococci. The NACP nanocomposite without NAg had CFU counts similar to, or slightly lower than, those of composite control. Even at the lowest NAg mass fraction of 0.028%, the CFU counts were reduced by 3-fold, compared to that without NAg. With 0.042% of NAg, the CFU counts were reduced by 4-fold, compared to that without NAg.

Figure 6 plots the lactic acid production by biofilms. The biofilms on the commercial composite control produced the most amount of acid. Adding NAg into the NACP composite progressively decreased the lactic acid production of the microcosm biofilms. Note that all the values in Figure 6 are significantly different ($p < 0.05$). At an intermediate 0.042% of NAg, the lactic acid production was reduced by nearly 3-fold, compared to that of composite control.

DISCUSSION

This study investigated the effect of silver nanoparticle mass fraction in NACP nanocomposite on dental plaque microcosm biofilms for the first time. There has been little study on the incorporation of antibacterial agents into Ca and PO_4 releasing dental composites. The addition of NAg into NACP composite greatly reduced the biofilm viability, metabolic activity, CFU counts, and lactic acid production. At NAg mass fraction

of 0.042%, the CFU counts and lactic acid were reduced to 20–30% of those for a commercial composite control. On the other hand, the flexural strength and elastic modulus of NACP composite were not decreased with 0.042% of NAg incorporation. Mechanical properties are important for composites for load-bearing restorations, because secondary caries and bulk fracture are cited as the two main reasons for restoration failure.[13,14] In the present study, the photo-cured NACP nanocomposite contained 35% of glass particles for reinforcement. As a result, its mechanical properties matched those of a commercial composite, which had neither Ca and PO_4 release nor antibacterial property.

Biofilm is a heterogeneous structure consisting of clusters of various types of bacteria embedded in an extracellular matrix. Cariogenic bacteria such as *S. mutans* and lactobacilli in the dental plaque can metabolize carbohydrates to acids, causing demineralization of the tooth and the tooth-restoration margins beneath the biofilm. Therefore, it is beneficial for the NACP composite with NAg to be able to hinder biofilm growth and acid production. Previous studies showed that the NACP composite released high levels of Ca and PO_4 ions[24] and neutralized cariogenic acid solutions.[25] The Ca and PO_4 releases were similar to those of previous studies which showed remineralization of tooth lesions.[20,22] Therefore, incorporating an antibacterial agent into the NACP nanocomposite is a promising method to combine three benefits, namely, remineralization, acid neutralization, and antibacterial capabilities.

An important method in previous studies was to use quaternary ammonium salts (QASs).[40–44] QASs have a potent antimicrobial activity and yet a low toxicity, and are often used in water treatment, surface coatings, and the food industry.[45] QASs include polymerizable monomers and non-polymerizable small molecules. QAS monomers can be copolymerized with dental resins by forming a covalent bond with the polymer network, leading to QAS immobilization in the composite. *S. mutans* growth was hindered on resins containing 12-methacryloyloxydodecylpyridinium bromide (MDPB).[46] A bonding system containing MDPB also possessed potent antibacterial activity.[41] Other investigators have synthesized resins containing methacryloxylethyl cetyl dimethyl ammonium chloride and cetylpyridinium chloride.[42,47] Another study developed antibacterial glass ionomer cements containing QAS bromides and chlorides.[43] In addition, QAS nanoparticles were prepared and incorporated into a dental composite.[48]

Another important antibacterial agent is Ag, which has been incorporated into dental composites with promising antibacterial properties.[28,29] Ag is antimicrobial against a wide range of micro-organisms.[30,49–51] Studies suggest that the antimicrobial mechanism is through Ag ions that inactivate the vital enzymes of bacteria, causing DNA in the bacteria to lose its replication ability, which leads to cell death.[30,51] One advantage of Ag is that it has good biocompatibility and low toxicity to human cells.[50] The second advantage is that Ag-containing composites have long-term antibacterial effects.[52] For example, one study showed that an Ag-containing composite inhibited *S. mutans* growth for more than 6 months.[29] The third advantage is that Ag causes less bacterial resistance than antibiotics.[53] The fourth advantage is that Ag nanoparticles with a small size and a high surface area can achieve antibacterial efficacy at a low filler level. A recent study developed a NAg nanoparticle-containing resin that showed significant antibacterial property at a NAg mass fraction of 0.08% in the resin.[32] That study did not examine the effect of different NAg mass fractions on antibacterial properties, and did not incorporate NAg into CaP composites.

In the present study, the NAg mass fraction was varied from 0.028–0.175% in the NACP nanocomposite. Since the Ag 2-ethylhexanoate salt did not dissolve in the hydrophobic BisGMA–TEGDMA monomers, it was first dissolved in TBAEMA monomer, which was then mixed with the BisGMA–TEGDMA resin. After the composite was photo-

polymerized, the Ag nanoparticles were well dispersed in the resin with a mean particle size of 2.7 nm. One merit of this method is that it enabled the Ag salt to be reduced to Ag nanoparticles *in situ* in the resin, thereby avoiding the need to mix pre-fabricated Ag nanoparticles with the resin which could cause agglomeration. The second merit is that the TBAEMA used to dissolve the Ag salt contains a reactive methacrylate functionality. Therefore, when the composite was photo-cured, the TBAEMA was chemically bonded with the polymer network.[32] NAg in the NACP nanocomposite imparted a substantial antibacterial capability, which increased with higher NAg content. When the NAg mass fraction was increased to 0.175%, the composite had a brownish color which was accompanied by a precipitous strength drop. Therefore, to maintain esthetics and mechanical strength, NAg mass fraction of higher than 0.042% should not be used. The nanocomposite containing 0.042% of NAg was able to greatly reduce biofilm metabolic activity, CFU counts and lactic acid production, compared to a commercial composite control.

Microcosms are laboratory models that are inoculated using material removed from the environment of interest, which maintain much of the complexity and heterogeneity of the original biological sample.[34] Dental biofilm models can be divided into three groups: single species, defined consortium, and microcosm[34]. *S. mutans* played a major role in dental caries and was widely used in single species biofilm models.[27] However, dental plaque is a complicated ecosystem with about 1000 different bacterial species.[54] Several studies used saliva from a single donor to grow plaque microcosm biofilms.[35,36,55,56] Other studies used a mixed saliva from different donors.[57,58] In dental plaque, streptococcal species plays an important role in the caries process, especially in the initial microflora.[59] Much research has suggested that mutans streptococci are the major pathogens of dental caries.[60] Hence, in the present study, three types of agar plates were used to test for total microorganisms, total streptococci, and mutans streptococci. All three CFU counts greatly decreased upon incorporation of NAg in NACP nanocomposite. The results suggest that the microcosm *biofilm model using human saliva as inoculum is a useful model for evaluating antibacterial composites*. Further study is needed to examine the NACP-NAg nanocomposite in an *in situ* model on its anti-biofilm and anti-caries efficacy.

CONCLUSIONS

The effects of silver nanoparticle mass fraction in NACP nanocomposite on mechanical properties and human plaque microcosm biofilm response were investigated for the first time. NACP of a particle size of 116 nm and NAg of a particle size of 2.7 nm were used in the resin composite. Flexural strength and elastic modulus of NACP nanocomposite with 0–0.042% of NAg matched those of a commercial composite with neither Ca and PO_4 release nor antibacterial activity. Incorporation of NAg into NACP nanocomposite greatly reduced the biofilm CFU counts, metabolic activity, and lactic acid production. The antibacterial potency significantly increased with higher NAg mass fraction. The strong antibacterial properties, together with the Ca and PO_4 release and acid neutralization capability shown previously, suggest that the novel NACP nanocomposite containing NAg is promising for caries-inhibiting restorations.

Acknowledgments

The authors thank Dr. L.C. Chow and Dr. L. Sun of the American Dental Association, Prof. Ashraf Fouad of the University of Maryland School of Dentistry, and Prof. Qianming Chen of the West China College of Stomatology for discussions. They are grateful to Esstech (Essington, PA) for donating the materials, and the Core Imaging Facility of University of Maryland Baltimore for technical support. This study was supported by NIH R01DE17974 and R01DE14190 (HX), a seed fund (HX) from the University of Maryland School of Dentistry, NIDCR-NIST Interagency Agreement Y1-DE-7005-01, NIST, and West China College of Stomatology.

Certain commercial materials and equipment are identified in this article to specify the experimental procedure. This does not implyrecommendation or endorsement by NIST or that the material or equipment identified is necessarily the best available for the purpose. Official contribution of the National Institute of Standards and Technology (NIST); not subject to copyright in the United States.

REFERENCES

1. Ferracane JL. Resin composite—State of the art. Dent Mater. 2011; 27:29–38. [PubMed: 21093034]
2. Bayne SC, Thompson JY, Swift EJ Jr, Stamatiades P, Wilkerson M. A characterization of first-generation flowable composites. J Am Dent Assoc. 1998; 129:567–577. [PubMed: 9601169]
3. Lim BS, Ferracane JL, Sakaguchi RL, Condon JR. Reduction of polymerization contraction stress for dental composites by two-step light-activation. Dent Mater. 2002; 18:436–444. [PubMed: 12098572]
4. Watts DC, Marouf AS, Al-Hindi AM. Photo-polymerization shrinkage-stress kinetics in resin-composites: Methods development. Dent Mater. 2003; 19:1–11. [PubMed: 12498890]
5. Lu H, Stansbury JW, Bowman CN. Impact of curing protocol on conversion and shrinkage stress. J Dent Res. 2005; 84:822–826. [PubMed: 16109991]
6. Xu X, Ling L, Wang R, Burgess JO. Formation and characterization of a novel fluoride-releasing dental composite. Dent Mater. 2006; 22:1014–1023. [PubMed: 16378636]
7. Drummond JL. Degradation, fatigue, and failure of resin dental composite materials. J Dent Res. 2008; 87:710–719. [PubMed: 18650540]
8. Svanberg M, Mjör IA, Ørstavik D. Mutans streptococci in plaque from margins of amalgam, composite, and glass-ionomer restorations. J Dent Res. 1990; 69:861–864. [PubMed: 2109000]
9. Imazato S, Torii M, Tsuchitani Y, McCabe JF, Russell RRB. Incorporation of bacterial inhibitor into resin composite. J Dent Res. 1994; 73:1437–1443. [PubMed: 8083440]
10. Zalkind MM, Keisar O, Ever-Hadani P, Grinberg R, Sela MN. Accumulation of Streptococcus mutans on light-cured composites and amalgam: An *in vitro* study. J Esthet Dent. 1998; 10:187–190. [PubMed: 9893513]
11. Beyth N, Domb AJ, Weiss E. An *in vitro* quantitative antibacterial analysis of amalgam and composite resins. J Dent. 2007; 35:201–206. [PubMed: 16996674]
12. Mjöor IA, Moorhead JE, Dahl JE. Reasons for replacement of restorations in permanent teeth in general dental practice. International Dent J. 2000; 50:361–366.
13. Sakaguchi RL. Review of the current status and challenges for dental posterior restorative composites: Clinical, chemistry, and physical behavior considerations. Dent Mater. 2005; 21:3–6. [PubMed: 15680996]
14. Sarrett DC. Clinical challenges and the relevance of materials testing for posterior composite restorations. Dent Mater. 2005; 21:9–20. [PubMed: 15680997]
15. Deligeorgi V, Mjor IA, Wilson NH. An overview of reasons for the placement and replacement of restorations. Prim Dent Care. 2001; 8:5–11. [PubMed: 11405031]
16. Frost PM. An audit on the placement and replacement of restorations in a general dental practice. Prim Dent Care. 2002; 9:31–36. [PubMed: 11901789]
17. NIDCR (National Institute of Dental and Craniofacial Research) announcement # 13-DE-102, Dental Resin Composites and Caries. 2009 Mar 5.
18. Jokstad A, Bayne S, Blunck U, Tyas M, Wilson N. Quality of dental restorations. FDI Commission Projects 2–95. International Dent J. 2001; 51:117–158.
19. Skrtic D, Antonucci JM, Eanes ED, Eichmiller FC, Schumacher GE. Physiological evaluation of bioactive polymeric composites based on hybrid amorphous calcium phosphates. J Biomed Mater Res B. 2000; 53:381–391.
20. Dickens SH, Flaim GM, Takagi S. Mechanical properties and biochemical activity of remineralizing resin-based Ca-PO_4 cements. Dent Mater. 2003; 19:558–566. [PubMed: 12837405]
21. Xu HHK, Sun L, Weir MD, Antonucci JM, Takagi S, Chow LC. Nano dicalcium phosphate anhydrous-whisker composites with high strength and Ca and PO_4 release. J Dent Res. 2006; 85:722–727. [PubMed: 16861289]

22. Langhorst SE, O'Donnell JN, Skrtic D. *In vitro* remineralization of enamel by polymeric amorphous calcium phosphate composite: Quantitative microradiographic study. Dent Mater. 2009; 25:884–891. [PubMed: 19215975]
23. Xu HHK, Weir MD, Sun L, Moreau JL, Takagi S, Chow LC, Antonucci JM. Strong nanocomposites with Ca, PO_4 and F release for caries inhibition. J Dent Res. 2010; 89:19–28. [PubMed: 19948941]
24. Xu HHK, Moreau JL, Sun L, Chow LC. Nanocomposite containing amorphous calcium phosphate nanoparticles for caries inhibition. Dent Mater. 2011; 27:762–769. [PubMed: 21514655]
25. Moreau JL, Sun L, Chow LC, Xu HHK. Mechanical and acid neutralizing properties and inhibition of bacterial growth of amorphous calcium phosphate dental nanocomposite. J Biomed Mater Res Part B. 2011; 98:80–88.
26. Monteiro DR, Gorup LF, Takamiya AS, Ruvollo-Filho AC, de Camargo ER, Barbosa DB. The growing importance of materials that prevent microbial adhesion: Antimicrobial effect of medical devices containing silver. Int J Antimicrob Agent. 2009; 34:103–110.
27. Allaker RP. The use of nanoparticles to control oral biofilm formation. J Dent Res. 2010; 89:1175–1186. [PubMed: 20739694]
28. Yamamoto K, Ohashi S, Aono M, Kokubo T, Yamada I, Yamauchi J. Antibacterial activity of silver ions implanted in SiO_2 filler on oral streptococci. Dent Mater. 1996; 12:227–229. [PubMed: 9002839]
29. Yoshida K, Tanagawa M, Atsuta M. Characterization and inhibitory effect of antibacterial dental resin composites incorporating silver-supported materials. J Biomed Mater Res. 1999; 4:516–522. [PubMed: 10497286]
30. Morones JR, Elechiguerra JL, Camacho A, Holt K, Kouri JB, Ramirez JT, Yacaman MJ. The bactericidal effect of silver nanoparticles. Nanotechnology. 2005; 16:2346–2353. [PubMed: 20818017]
31. Fan C, Chu L, Rawls HR, Norling BK, Cardenas HL, Whang K. Development of an antimicrobial resin - A pilot study. Dent Mater. 2011; 27:322–328. [PubMed: 21112619]
32. Cheng YJ, Zeiger DN, Howarter JA, Zhang X, Lin NJ, Antonucci JM, Lin-Gibson S. *In situ* formation of silver nanoparticles in photocrosslinking polymers. J Biomed Mater Res B. 2011; 97:124–131.
33. Lee Y, Lu H, Oguri M, Powers JM. Changes in gloss after simulated generalized wear of composite resins. J Prosthet Dent. 2005; 94:370–376. [PubMed: 16198175]
34. McBain AJ. *In vitro* biofilm models: An overview. Adv Appl Microbiol. 2009; 69:99–132. [PubMed: 19729092]
35. Cheng L, Exterkate RA, Zhou X, Li J, ten Cate JM. Effect of galla chinensis on growth and metabolism of microcosm biofilms. Caries Res. 2011; 45:87–92. [PubMed: 21346356]
36. McBain AJ, Sissons C, Ledder RG, Sreenivasan PK, De Vizio W, Gilbert P. Development and characterization of a simple perfused oral microcosm. J Appl Microbiol. 2005; 98:624–634. [PubMed: 15715865]
37. Lima JP, Sampaio de Melo MA, Borges FM, Teixeira AH, Steiner-Oliveira C, Nobre Dos Santos M, Rodrigues LK, Zanin IC. Evaluation of the antimicrobial effect of photodynamic antimicrobial therapy in an in situ model of dentine caries. Eur J Oral Sci. 2009; 117:568–574. [PubMed: 19758254]
38. Gold OG, Jordan HV, Van Houte J. A selective medium for Streptococcus mutans. Arch Oral Biol. 1973; 18:1357–1364. [PubMed: 4518755]
39. van Loveren C, Buijs JF, ten Cate JM. The effect of triclosan toothpaste on enamel demineralization in a bacterial demineralization model. J Antimicrob Chemother. 2000; 45:153–158. [PubMed: 10660496]
40. Imazato S. Review: Antibacterial properties of resin composites and dentin bonding systems. Dent Mater. 2003; 19:449–457. [PubMed: 12837391]
41. Imazato S. Bioactive restorative materials with antibacterial effects: New dimension of innovation in restorative dentistry. Dent Mater J. 2009; 28:11–19. [PubMed: 19280964]

42. Li F, Chen J, Chai Z, Zhang L, Xiao Y, Fang M, Ma S. Effects of a dental adhesive incorporating antibacterial monomer on the growth, adherence and membrane integrity of Streptococcus mutans. J Dent. 2009; 37:289–296. [PubMed: 19185408]
43. Xie D, Weng Y, Guo X, Zhao J, Gregory RL, Zheng C. Preparation and evaluation of a novel glass-ionomer cement with antibacterial functions. Dent Mater. 2011; 27:487–496. [PubMed: 21388668]
44. Tezvergil-Mutluay A, Agee KA, Uchiyama T, Imazato S, Mutluay MM, Cadenaro M, Breschi L, Nishitani Y, Tay FR, Pashley DH. The inhibitory effects of quaternary ammonium methacrylates on soluble and matrix-bound MMPs. J Dent Res. 2011; 90:535–540. [PubMed: 21212315]
45. Kourai H, Yabuhara T, Sjirai A, Maeda T, Nagamune H. Syntheses and antimicrobial activities of a series of new bis-quaternary ammonium compounds. Eur J Med Chem. 2006; 41:437–444. [PubMed: 16517025]
46. Thome T, Mayer MPA, Imazato S, Geraldo-Martins VR, Marques MM. *In vitro* analysis of inhibitory effects of the antibacterial monomer MDPB-containing restorations on the progression of secondary root caries. J Dent. 2009; 37:705–711. [PubMed: 19540033]
47. Namba N, Yoshida Y, Nagaoka N, Takashima S, Matsuura-Yoshimoto K, Maeda H, Van Meerbeek B, Suzuki K, Takashida S. Antibacterial effect of bactericide immobilized in resin matrix. Dent Mater. 2009; 25:424–430. [PubMed: 19019421]
48. Beyth N, Yudovin-Farber I, Bahir R, Domb AJ, Weiss EI. Antibacterial activity of dental composites containing quaternary ammonium polyethylenimine nanoparticles against Streptococcus mutans. Biomaterials. 2006; 27:3995–4002. [PubMed: 16564083]
49. Li P, Li J, Wu C, Wu Q, Li J. Synergistic antibacterial effects of β-lactam antibiotic combined with silver nanoparticles. Nanotechnology. 2005; 16:1912–1917.
50. Slenters TV, Hauser-Gerspach I, Daniels AU, Fromm KM. Silver coordination compounds as light-stable, nano-structured and anti-bacterial coatings for dental implant and restorative materials. J Mater Chem. 2008; 18:5359–5362.
51. Rai M, Yada A, Gade A. Silver nanoparticles as a new generation of antimicrobials. Biotechnol Adv. 2009; 27:76–83. [PubMed: 18854209]
52. Damm C, Munsted H, Rosch A. Long-term antimicrobial polyamide 6/silver nanocomposites. J Mater Sci. 2007; 42:6067–6073.
53. Percival SL, Bowler PG, Russell D. Bacterial resistance to silver in wound care. J Hospital Infect. 2005; 60:1–7.
54. ten Cate JM. Biofilms, a new approach to the microbiology of dental plaque. Odontology. 2006; 94:1–9. [PubMed: 16998612]
55. Cenci MS, Pereira-Cenci T, Cury JA, Ten Cate JM. Relationship between gap size and dentine secondary caries formation assessed in a microcosm biofilm model. Caries Res. 2009; 43:97–102. [PubMed: 19321986]
56. Wong L, Sissons CH. Human dental plaque microcosm biofilms: Effect of nutrient variation on calcium phosphate deposition and growth. Arch Oral Biol. 2007; 52:280–289. [PubMed: 17045564]
57. Badawi H, Evans RD, Wilson M, Ready D, Noar JH, Pratten J. The effect of orthodontic bonding materials on dental plaque accumulation and composition in vitro. Biomaterials. 2003; 24:3345–3350. [PubMed: 12763461]
58. Pratten J, Wilson M, Spratt DA. Characterization of in vitro oral bacterial biofilms by traditional and molecular methods. Oral Microbiol Immunol. 2003; 18:45–49. [PubMed: 12588458]
59. Li J, Helmerhorst EJ, Leone CW, Troxler RF, Yaskell T, Haffajee AD, Socransky SS, Oppenheim FG. Identification of early microbial colonizers in human dental biofilm. J Appl Microbiol. 2004; 97:1311–1318. [PubMed: 15546422]
60. Takahashi N, Nyvad B. Caries ecology revisited: Microbial dynamics and the caries process. Caries Res. 2008; 42:409–418. [PubMed: 18832827]

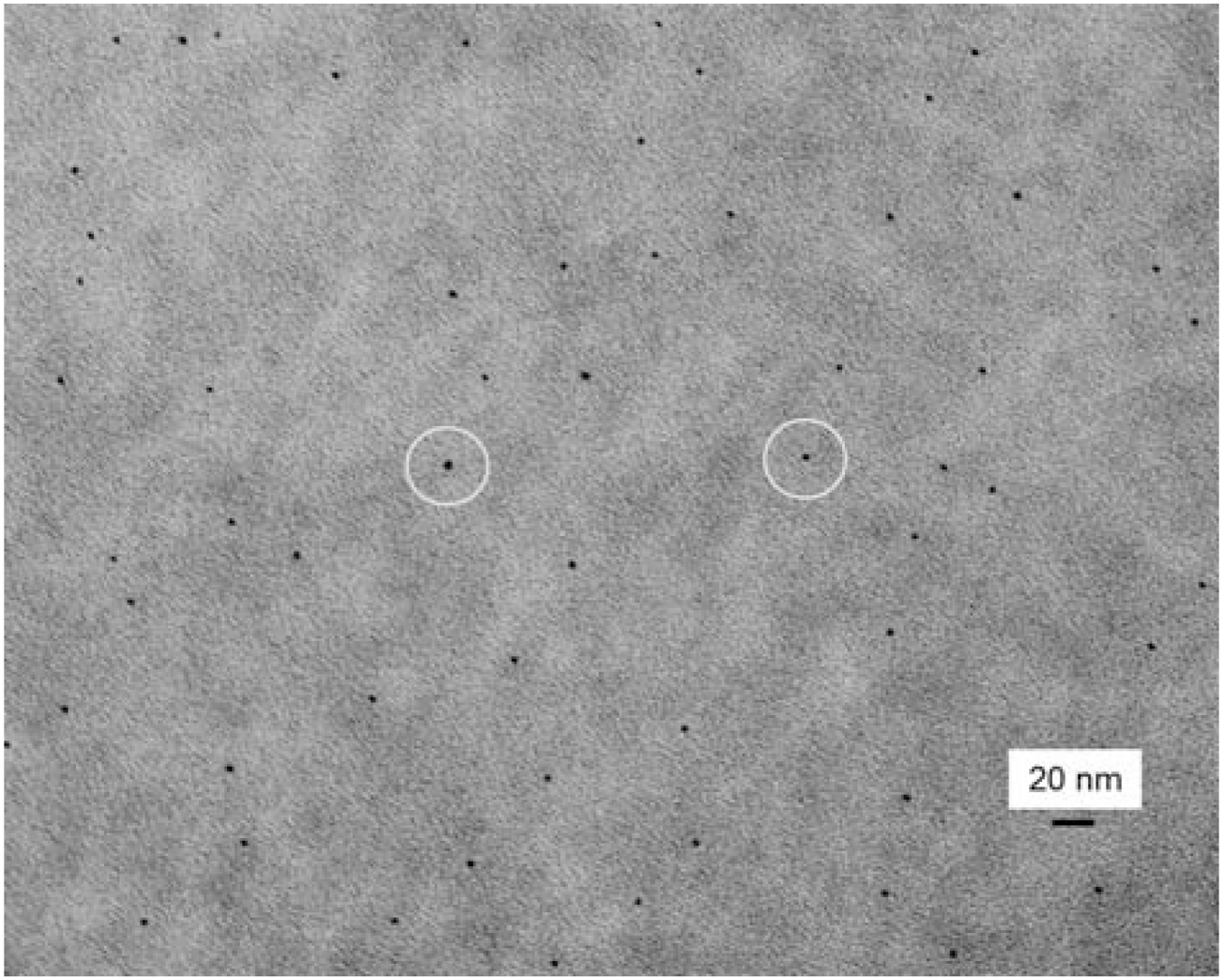

FIGURE 1.

Representative TEM image of nanoparticles of silver (NAg) in the BisGMA-TEGDMA resin. This example used 0.08% mass fraction of Ag salt in the resin. The NAg particles appeared as black dots, with examples indicated by the circles. The particle size for NAg (mean ± sd; $n = 100$) was measured to be (2.7 ± 0.6) nm. The NAg particles were well dispersed in the resin matrix. [Color figure can be viewed in the online issue, which is available at wileyonlinelibrary.com.]

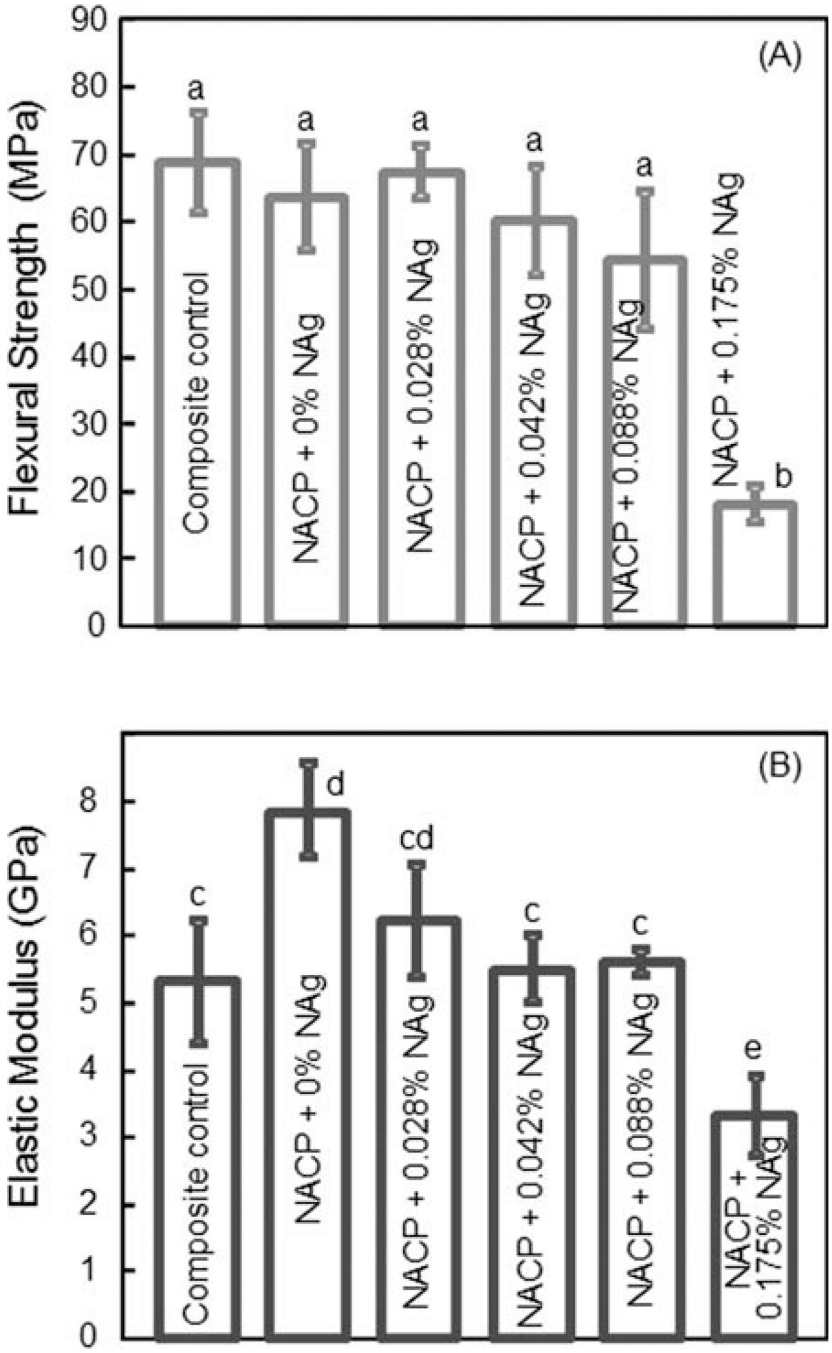

FIGURE 2.

Mechanical properties of NACP nanocomposites containing NAg: (A) Flexural strength, and (B) elastic modulus. Each value is the mean of six measurements with the error bar showing one standard deviation (mean ± sd; $n = 6$). In each plot, values with dissimilar letters are significantly different ($p < 0.05$). [Color figure can be viewed in the online issue, which is available at wileyonlinelibrary.com.]

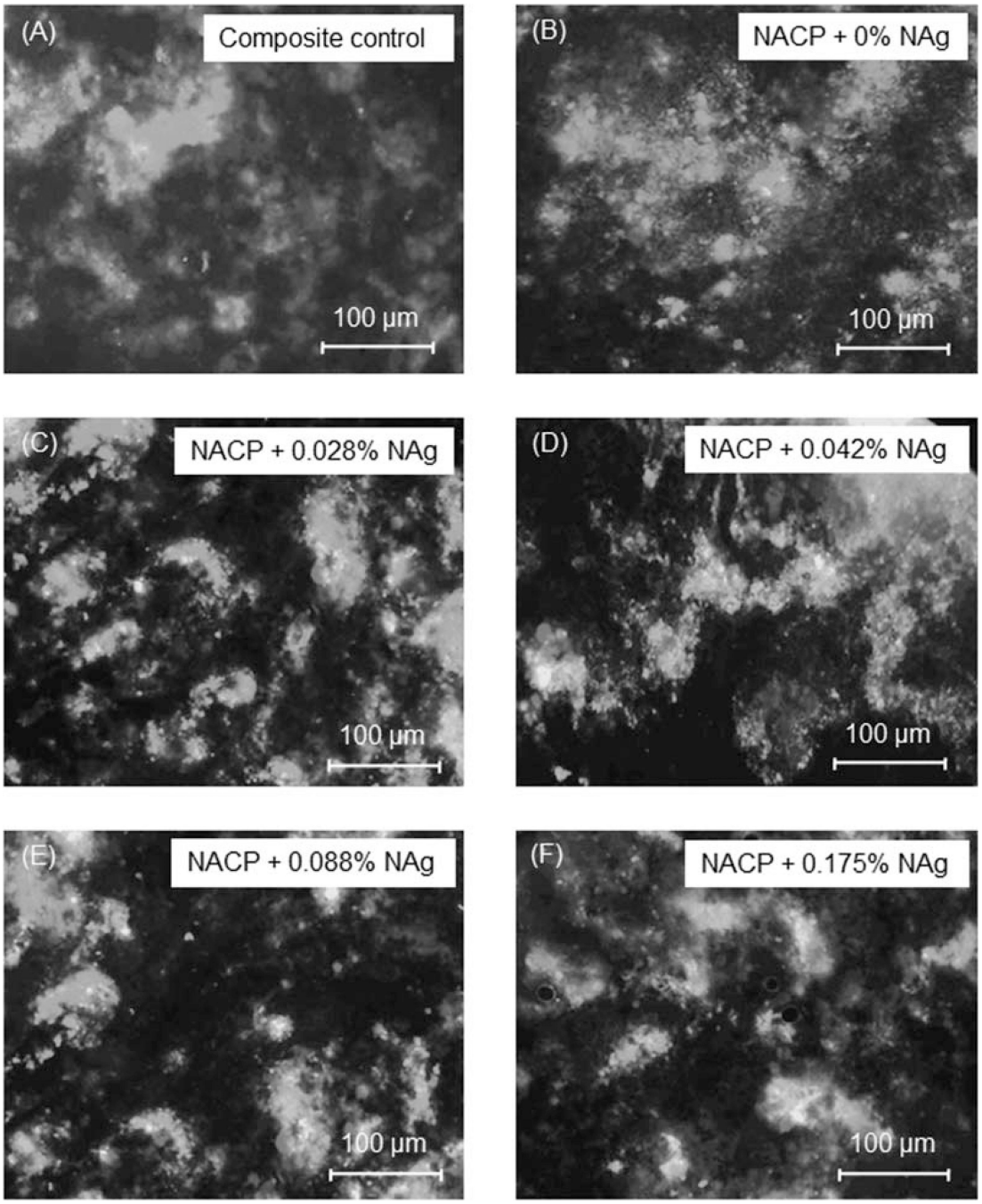

FIGURE 3.

Live/dead images of dental plaque microcosm biofilms at 48 h on six types of composites. Live bacteria were stained green, and dead bacteria were stained red. Yellow/orange colors appeared when the live and dead bacteria were in close proximity. Note that the antibacterial potency increased with higher NAg content, with a noticeable increase in the red/orange staining colors. [Color figure can be viewed in the online issue, which is available at wileyonlinelibrary.com.]

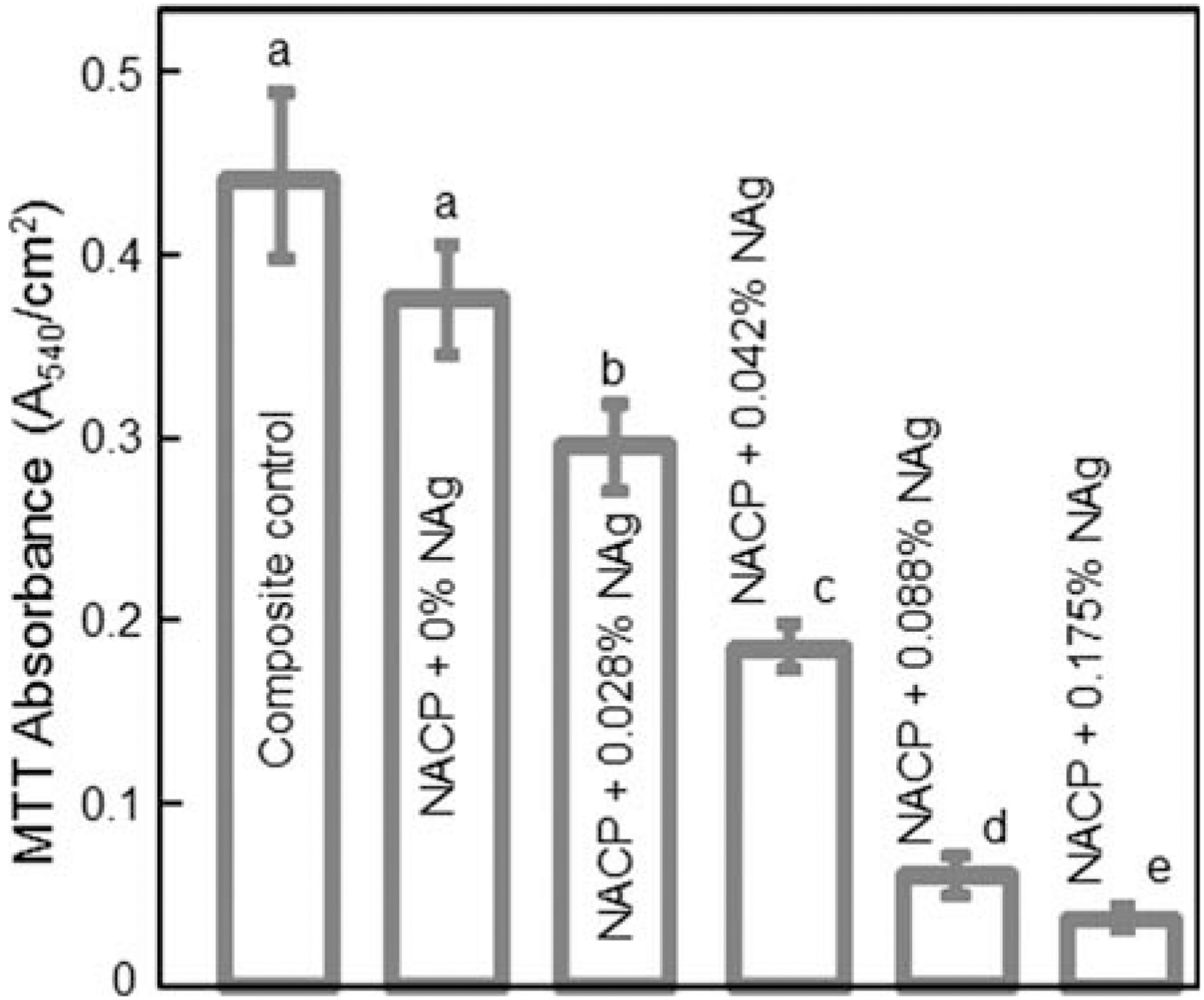

FIGURE 4.

MTT metabolic activity of 48 h biofilms on composites. Each value is mean ± sd; $n = 6$. Values with dissimilar letters are significantly different ($p < 0.05$). The metabolic activity on NACP nanocomposite with NAg was markedly reduced when compared to the NACP nanocomposite without NAg, as well as to the commercial composite control. [Color figure can be viewed in the online issue, which is available at wileyonlinelibrary.com.]

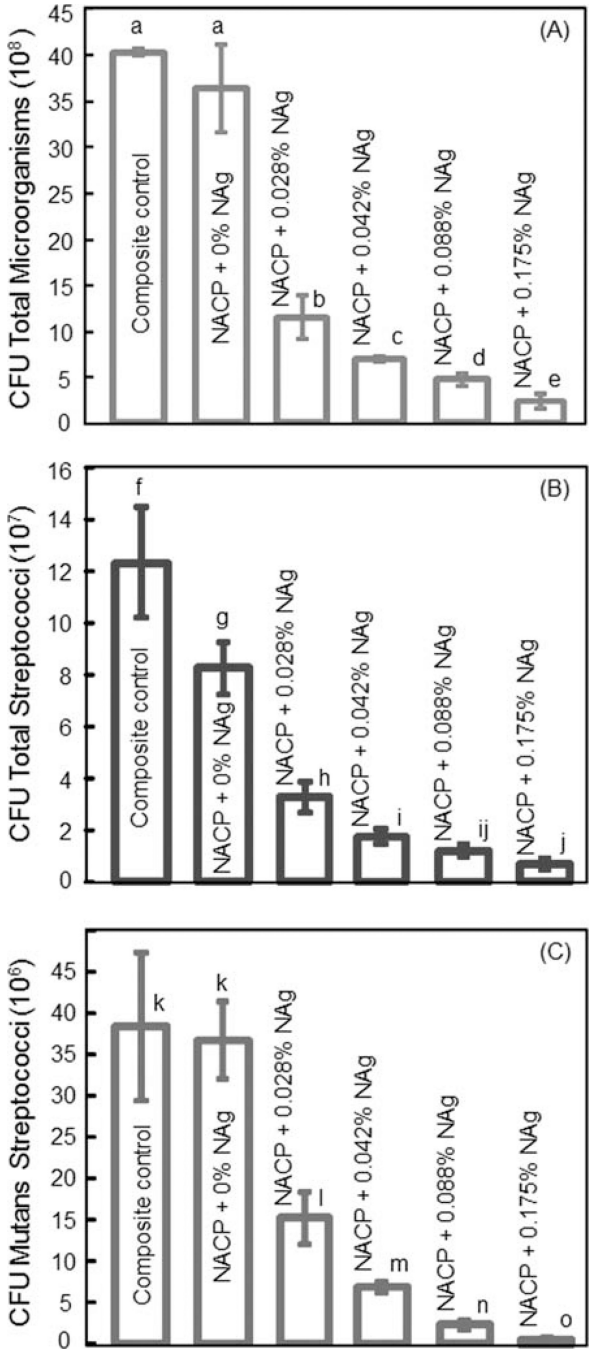

FIGURE 5.

Colony-forming unit (CFU) counts for 48 h biofilms on the six types of composites: (A) Total microorganisms, (B) total Streptococci, and (C) mutans Streptococci. Each value is mean ± sd; $n = 6$. In each plot, values with dissimilar letters are significantly different ($p < 0.05$). The CFU counts on NACP nanocomposite with NAg was much lower than those on the NACP nanocomposite without NAg and the commercial composite control. [Color figure can be viewed in the online issue, which is available at wileyonlinelibrary.com.]

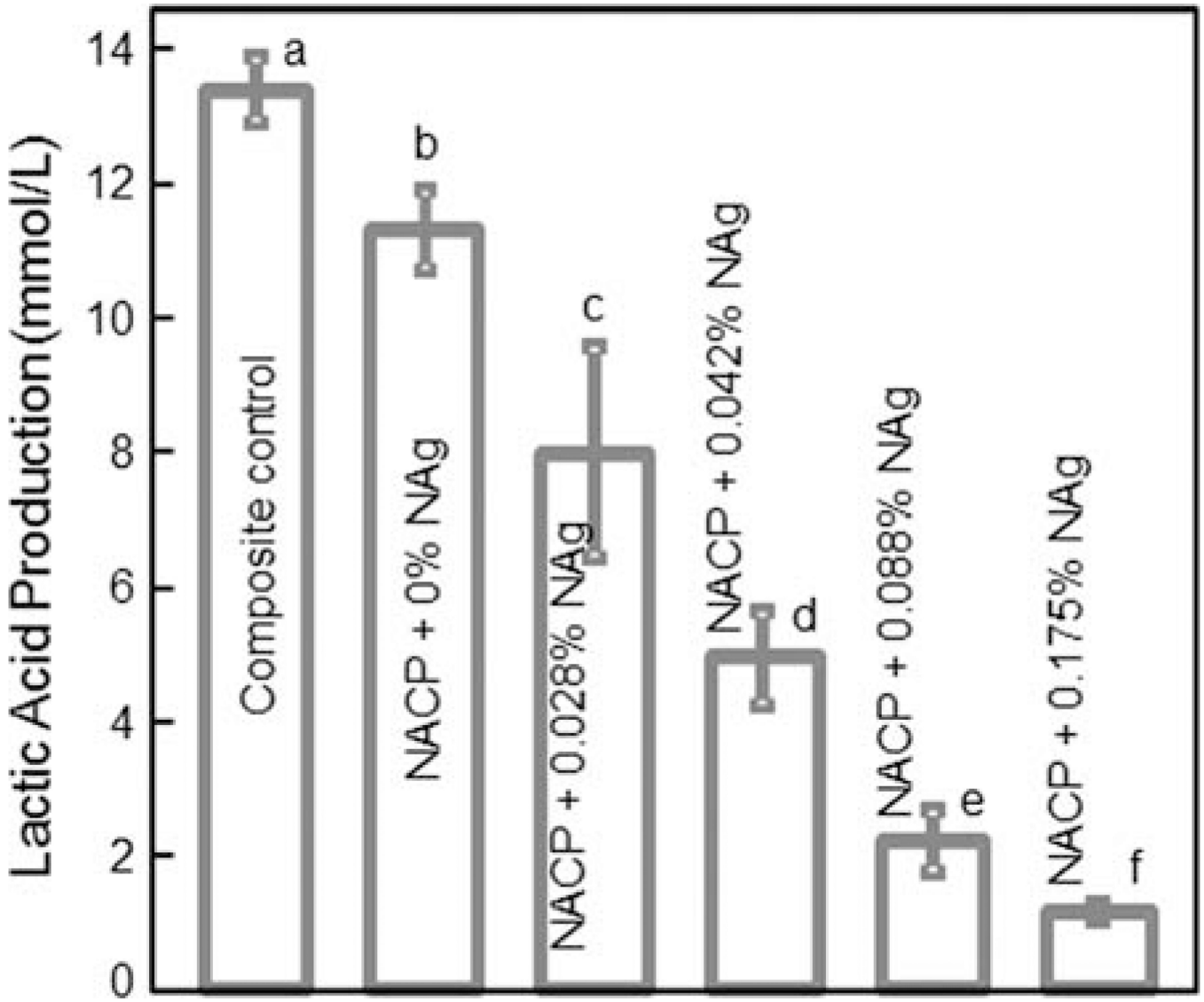

FIGURE 6.

Lactic acid production by 48 h biofilms on composites. Each value is mean ± sd; $n = 6$. Values with dissimilar letters are significantly different ($p < 0.05$). The dental plaque microcosm biofilms on the NACP nanocomposite with NAg produced far less acid than the biofilms on the composites without NAg or on the commercial composite control. [Color figure can be viewed in the online issue, which is available at wileyonlinelibrary.com.]